ISBN: 978-628-96613-3-0. ISSN: 2414-6390. Digital Object Identifier: https://dx.doi.org/10.18687/LACCEI2026.1.1.1872

Comparative Braking Performance of OEM, OE, and IAM Brake Pads on a Light SUV Under Loaded and Unloaded Conditions

Erasmo García, Mgtr[1], Daniel Cevallos, Mgtr[2], Henry Friend, BSc[3], Sahel Tapuy, Mgtr [4], José Torres, Mgtr [5], Holger Cevallos, PhD [6] and Miguel Torres, PhD[7]
[2,4,6,7]Escuela Superior Politécnica del Litoral, ESPOL, Ecuador, Facultad de Ingeniería en Electricidad y Computación (FIEC), Ecuador, dacevall@espol.edu.ec, stapuy@espol.edu.ec, hcevallo@espol.edu.ec, mitorres@espol.edu.ec
[1,3,5]Universidad Internacional del Ecuador UIDE, Quito 170411, Ecuador, ergarcia@uide.edu.ec, hefriendmo@uide.edu.ec, jostorresgo@uide.edu.ec

***Abstract*—Brake pad selection impacts safety, stopping performance, and thermal behavior, especially when vehicle mass and usage conditions vary. This paper presents a controlled road-test comparison of three disc brake pad categories—Original Equipment Manufacturer (OEM), Original Equipment (OE), and Independent Aftermarket (IAM)—installed on the same light sport utility vehicle and evaluated under two load states (unloaded and loaded). Commercial brand/model names are withheld for confidentiality; therefore, pads are reported by category with supply-chain and market-tier context. Each configuration was tested with five repeated full stops from a nominal initial speed of 90 km h^{-1} on dry asphalt, capturing stopping time and distance, peak brake-pad temperatures (front/rear), and peak hydraulic line pressures (front/rear). Results are reported as mean $\pm$ standard deviation and complemented with variability metrics. Across all tests, loading increased stopping distance and time, and relative performance depended on pad category. Under unloaded conditions, the OEM configuration achieved the shortest mean stopping distance (25.03 m) and time (2.00 s), while OE and IAM exhibited longer stops. Under loaded conditions, OEM and OE were comparable in distance and time, whereas IAM showed a larger degradation. The dataset supports a repeatable, instrumentation-driven workflow for pad benchmarking and highlights the importance of reporting dispersion—not only averages—when assessing braking components.**

***Index Terms*—Brake pads, stopping distance, stopping time, OEM, aftermarket, hydraulic pressure, brake temperature, vehicle testing.**

I. Introduction

Stopping distance is a primary safety metric for light vehicles and is influenced by tire–road friction, brake system capability, vehicle loading, and the thermal behavior of friction materials [1], [2], [3], [4]. In many emerging markets, brake-pad purchases are driven primarily by price and availability rather than certified performance. In Ecuador in particular, consumers may face limited labeling, scarce information about authorized brands, and uneven quality control across the aftermarket supply chain. This motivates transparent, instrumentation-driven comparisons that report not only average stopping distance but also variability and thermal/hydraulic behavior under representative loading. Brake pads are commonly sold in three practical categories: OEM (manufacturer-specified), OE (supplier-grade replacements marketed as equivalent), and IAM (independent aftermarket). While IAM products may offer cost advantages, their friction stability with temperature and their interaction with the hydraulic system can vary, affecting both performance and repeatability [3], [5], [6].

Industry and regulatory test procedures emphasize controlled initial speed, straight-line braking, and repeatability, often requiring multiple repetitions and speed correction when initial-speed tolerance is exceeded [1], [7]. In addition, dynamometer-based standards (e.g., ISO and SAE procedures) motivate systematic assessment of friction behavior versus pressure, temperature, and speed [8], [9]. Brake lining temperature prior to each stop and maximum temperatures during stops are monitored because temperature is strongly coupled to friction coefficient, fade, and recovery [5], [7].

A. Related Work and Positioning

Prior studies have compared brake pads using material-level, dynamometer, and market-oriented methodologies. Balaji et al. evaluated four OEM brake pads for passenger cars using tribological tests and multi-criteria ranking, including performance coefficient of friction, hot coefficient of friction, fade, recovery, wear, and time to maximum temperature [10]. Neis et al. focused specifically on original and aftermarket brake pads sold in the Brazilian market, which is directly relevant to the present distinction between manufacturer-specified and replacement products [11], [12]. Sethupathi et al. analyzed disc brake pads sold in the Indian market from safety and environmental perspectives, and Omar et al. reported variability in composition and price relationships among Malaysian aftermarket pads [13], [14]. Together, these works show that market category and price alone do not fully characterize braking performance.

Other authors have emphasized the mechanisms behind these market-level differences. Kchaou et al. discuss the difficulty of interpreting friction behavior because the reported coefficient depends on test method, operating pressure, temperature, and speed [15]. Eriksson et al. further show that environmental conditions can affect brake-pad friction and noise behavior [16]. This paper complements those studies by moving from material or dynamometer characterization to controlled vehicle-level stops. In contrast with bench tests, the present road-test workflow includes the vehicle ABS, tire–road interface, load transfer, hydraulic pressure response, and IMU-measured deceleration signatures. Therefore, the contribution is not only to rank pad categories but also to connect pad choice with vehicle-level outcomes under representative loaded and unloaded service conditions.

B. Contributions

This work contributes:

- A repeatable road-test workflow aligned with SAE stopping-distance practices (test design, repetition, and data reduction).
- A comparative dataset (3 pad categories $\times$ 2 load states $\times$ 5 repetitions) including stopping distance/time, pad temperatures, and hydraulic pressures.
- A variability-focused analysis (standard deviation, coefficient of variation, and confidence intervals) to support component benchmarking beyond averages.

II. Experimental Setup and Methodology

A. Vehicle and Brake Configurations

The tests were conducted on a single light SUV (2009 Hyundai Santa Fe CRDI 2.2) equipped with four-wheel disc brakes and ABS. Using one vehicle avoided confounding effects from different brake hardware, tire types, suspension settings, or vehicle mass distributions. Three pad categories were evaluated:

- **OEM**: manufacturer-specified service pads for the vehicle model.
- **OE**: supplier-grade replacement pads from a first-tier supply-chain provider and marketed as equivalent to OEM.
- **IAM**: independent aftermarket pads from a budget-oriented brand available through local retail channels.

Commercial names, part numbers, and brand identifiers are not disclosed due to confidentiality restrictions in the test campaign and to avoid implying endorsement or negative identification of specific products. The reported categories describe the procurement channel and market tier, not a universal quality label. Therefore, the comparison should be interpreted as category-level evidence for the tested samples rather than as a public ranking of named brands. Each pad category was installed on both axles and tested under:

1) **Unloaded**: driver and instrumentation only, with no additional ballast beyond the measurement system.
2) **Loaded**: an added payload of approximately 300 kg, distributed as 200 kg in the rear cargo area and 100 kg in the front cabin to represent a realistic passenger/cargo service condition.

TABLE I: IMU/GNSS logging module capabilities (vendor datasheet).

Capability	Notes
Tri-axial acceleration	X, Y, Z axes
Tri-axial angular rate	X, Y, Z axes (gyroscope)
Attitude angles	roll/pitch/yaw from onboard fusion
Output rate	configurable up to $\sim$200 Hz
Interface	TTL serial (default 9600 baud)

B. Instrumentation

To characterize performance and thermal/hydraulic behavior, the setup recorded:

- Stopping time and stopping distance per stop.
- Peak brake-pad temperature (front/rear) during the stop.
- Peak hydraulic line pressure at the front and rear calipers during the stop.

Data were collected via an embedded acquisition system and exported for logging and post-processing. The instrumentation included pressure transducers installed in the brake hydraulic circuit, type-K thermocouples placed at the pad locations, and an IMU for dynamic response. Before each test series, the acquisition channels were checked for stable readings and cable routing was inspected to prevent contact with moving components. Signals were logged at 100 Hz, which was sufficient for the stop-duration and peak-value metrics reported in this study.

In addition, a compact 9-DOF IMU/GNSS module (WitMotion) logged tri-axial acceleration and angular rates to characterize the transient longitudinal dynamics during braking (Sec. IV-D). Table I summarizes key capabilities reported by the vendor [17].

C. Test Procedure

The road-test procedure follows the structure of SAE stopping-distance practices [1], [2]:

1) Accelerate in a straight line to a nominal $90\,\mathrm{km\,h^{-1}}$.
2) Apply full braking to a complete stop while maintaining a straight trajectory.
3) Record stopping time, stopping distance, peak temperatures, and peak pressures.
4) Before each series, verify tire pressure consistency, measure pavement temperature, and confirm correct acquisition of pressure/temperature/IMU streams.
5) Inspect cable routing to avoid wheel contact and ensure sensor integrity during the run.
6) Repeat $n = 5$ stops per configuration, using a minimum cooling interval of five minutes between stops to maintain comparable initial thermal conditions.

III. Data Reduction and Performance Metrics

A. Primary Metrics

For each stop i, the primary metrics are:

$$d_i = \text{stopping distance (m)}, \tag{1}$$

$$t_i = \text{stopping time (s)}, \tag{2}$$

Fig. 1: Controlled test environment for straight-line stops on dry asphalt.

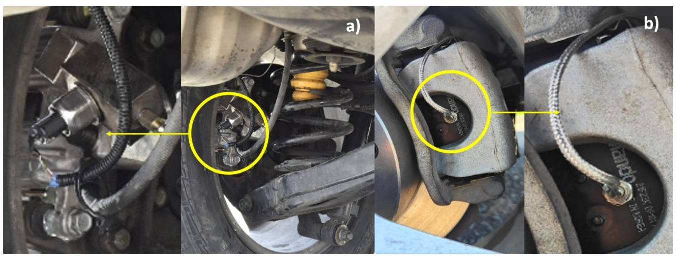

Fig. 2: Instrumentation used to record pressure and temperature signals during braking.

and the peak values measured during the stop:

$$T_{f,i},\ T_{r,i} = \text{front/rear peak pad temperature (°C)}, \quad (3)$$

$$P_{f,i},\ P_{r,i} = \text{front/rear peak hydraulic pressure (psi)}. \quad (4)$$

B. Speed Correction (When Applicable)

When the achieved initial speed differs from a target speed, SAE guidance commonly applies a quadratic correction [1], [7]:

$$d_{\text{corr}} = d_{\text{test}} \left(\frac{V_{\text{target}}}{V_{\text{test}}} \right)^2 . \quad (5)$$

In this dataset, the recorded initial speed was nominally constant across repetitions; therefore, results are reported without additional correction.

C. Dispersion and Repeatability

For each configuration, we report the sample mean $\bar{x}$ and sample standard deviation s over $n = 5$ repetitions. To quantify repeatability, we compute the coefficient of variation (CV) and the 95% confidence interval (CI) half-width:

$$\text{CV}(x) = 100\, \frac{s}{\bar{x}}, \quad (6)$$

$$\text{CI}_{95}(x) = t_{0.975,\, n-1}\, \frac{s}{\sqrt{n}}, \quad (7)$$

where $t_{0.975,\, n-1}$ is the Student-t critical value [18].

Fig. 3: Loaded condition setup used to represent an increased vehicle mass state.

IV. Results

The results are organized to match the study objectives: compare stopping performance among pad categories, quantify the effect of loading, characterize thermal and hydraulic behavior, and report repeatability rather than averages alone.

A. Summary Statistics

Table II reports mean $\pm$ standard deviation for all measured metrics.

B. Equivalent Deceleration and Effective Friction

For an initial speed $V_0 = 90\,\text{km}\,\text{h}^{-1}$ ($25\,\text{m}\,\text{s}^{-1}$), an equivalent constant-deceleration estimate can be derived from the mean stopping distance $\bar{d}$ as

$$a_{\text{eq}} = \frac{V_0^2}{2\,\bar{d}}, \quad (8)$$

and the corresponding effective friction level is $\mu_{\text{eq}} = a_{\text{eq}}/g$. These derived values provide an additional, interpretable summary of braking "severity" and are consistent with the reported distance/time means when speed is tightly controlled. Because they are computed from vehicle-level stopping distance, they should be treated as comparative effective indices rather than direct friction coefficients of the pad material.

C. Stopping Distance and Time

Fig. 4 reports mean stopping distance and time (mean $\pm$ SD, $n = 5$). Under unloaded conditions, OEM produced the shortest mean distance and time. Relative to OEM, OE increased the mean stopping distance by 3.20 m (+12.8%) and IAM by 6.59 m (+26.3%). The same pattern was observed for stopping time, where OE and IAM were longer than OEM by 13.2% and 26.4%, respectively. Under loaded conditions, OEM and OE were nearly equivalent in distance and time (OE: +0.5% in distance and +0.8% in time versus OEM), whereas IAM remained the longest-stopping configuration (+12.4% in distance and +12.5% in time versus OEM). Loading increased the mean distance for all categories: OEM by 7.98 m, OE by 4.93 m, and IAM by 5.48 m. These results directly address the objective of identifying whether category-level pad selection changes vehicle-level braking behavior under realistic mass variation.

TABLE II: Performance summary (mean $\pm$ SD, $n = 5$ stops) for each pad category and load state at nominal $90\,\mathrm{km\,h^{-1}}$.

Pad	Load	t (s)	d (m)	T_f (°C)	T_r (°C)	P_f (psi)	P_r (psi)
OEM	Unloaded	2.00 $\pm$ 0.21	25.03 $\pm$ 2.63	76.48 $\pm$ 1.01	70.23 $\pm$ 1.59	2190 $\pm$ 22	1330 $\pm$ 74
OE	Unloaded	2.27 $\pm$ 0.13	28.23 $\pm$ 1.63	81.73 $\pm$ 11.00	68.61 $\pm$ 11.02	2203 $\pm$ 14	1287 $\pm$ 92
IAM	Unloaded	2.53 $\pm$ 0.17	31.62 $\pm$ 2.18	71.87 $\pm$ 5.85	64.14 $\pm$ 5.87	2194 $\pm$ 32	1308 $\pm$ 82
OEM	Loaded	2.64 $\pm$ 0.17	33.01 $\pm$ 2.18	83.51 $\pm$ 5.08	77.92 $\pm$ 3.29	2197 $\pm$ 22	1522 $\pm$ 248
OE	Loaded	2.66 $\pm$ 0.14	33.16 $\pm$ 1.96	135.62 $\pm$ 26.30	116.97 $\pm$ 26.76	2157 $\pm$ 87	1610 $\pm$ 187
IAM	Loaded	2.97 $\pm$ 0.17	37.10 $\pm$ 2.15	91.35 $\pm$ 9.94	85.46 $\pm$ 7.35	2181 $\pm$ 29	1760 $\pm$ 210

TABLE III: Equivalent constant-deceleration estimates derived from mean stopping distance ($V_0 = 90\,\mathrm{km\,h^{-1}}$).

Pad	Load	$\bar{d}$ (m)	a_{eq} (m/s^2)	μ_{eq}
OEM	U	25.03	12.49	1.27
OE	U	28.23	11.07	1.13
IAM	U	31.62	9.88	1.01
OEM	L	33.01	9.47	0.97
OE	L	33.16	9.42	0.96
IAM	L	37.10	8.42	0.86

TABLE IV: Relative change versus OEM (mean) for each load state. Positive values indicate worse (longer) stops than OEM.

Pad	Load	Δd vs. OEM	Δt vs. OEM
OE	Unloaded	+12.8%	+13.2%
IAM	Unloaded	+26.3%	+26.4%
OE	Loaded	+0.5%	+0.8%
IAM	Loaded	+12.4%	+12.5%

Beyond mean values, Fig. 5 highlights the distribution across repetitions, which is important for safety-critical comparisons where repeatability matters.

D. Longitudinal Acceleration Profiles

To complement distance/time metrics, we analyzed the longitudinal acceleration signal during each full-stop event. The IMU reports acceleration as AccX in units of g, which can be converted to SI units via

$$a_x = g\,\mathrm{AccX}, \tag{9}$$

where $g \approx 9.81\,\mathrm{m\,s^{-2}}$. Negative a_x corresponds to vehicle deceleration.

Fig. 6 overlays representative acceleration traces for OEM, OE, and IAM under unloaded and loaded tests. Across conditions, braking produces a short transient followed by a deceleration plateau. Sharp spikes and high-frequency oscillations are consistent with ABS modulation and road/tire disturbances. Fig. 7 isolates the load effect for each pad category. The loaded case generally extends the deceleration duration, reflecting the higher kinetic energy that must be dissipated, while the plateau magnitude remains bounded by available tire–road friction and brake system limits.

E. Thermal and Hydraulic Behavior

Pad temperature provides a proxy for frictional energy dissipation and potential fade. Fig. 8 summarizes peak pad temperatures at the front and rear axles. OE showed the highest peak temperatures under loaded tests (front: 135.62 °C; rear: 116.97 °C), even though its loaded stopping distance and time were close to OEM. This means that similar stopping performance can be achieved with different thermal signatures, which is relevant for the objective of evaluating not only stopping distance but also operating severity. Fig. 9 reports peak hydraulic pressures. Front-axle pressures were broadly comparable across pad categories (approximately 2157–2203 psi), but rear pressures increased and became more variable under load, especially for IAM (1760 ± 210 psi). This pattern suggests that load transfer and ABS modulation influenced rear-axle hydraulic demand during high-deceleration stops.

V. Discussion

A. Effect of Loading

As expected, adding payload increased stopping distance and time for all pad categories, consistent with the increased kinetic energy that must be dissipated in each stop [3]. Table III expresses the same trend in terms of equivalent deceleration: unloaded OEM achieved the highest a_{eq}, while IAM under load exhibited the lowest a_{eq}. The load effect should be interpreted in two complementary ways. First, as a within-pad change, the absolute distance increase from unloaded to loaded conditions was 7.98 m for OEM, 4.93 m for OE, and 5.48 m for IAM. Second, as a between-pad comparison under the same loaded condition, IAM remained the weakest configuration, with a +12.4% longer distance and +12.5% longer time than OEM. This distinction avoids overinterpreting the load penalty and shows that the IAM configuration provided the lowest effective deceleration margin in the higher-energy loaded stop.

B. Thermal Response and Potential Fade Indicators

Peak temperatures increased under load, with OE showing the highest peaks. High temperatures do not necessarily imply worse performance; however, they can indicate different heat generation and dissipation characteristics and can influence friction stability and wear [5]. The observed combination of comparable stopping distance (OE vs. OEM in loaded state) but substantially higher pad temperatures suggests the need for complementary endurance and fade tests (e.g., repeated high-energy stops) before concluding equivalence.

C. Dynamic Braking Signatures from the IMU

The longitudinal acceleration profiles (Figs. 6–7) provide an interpretable signature of how each pad category engages

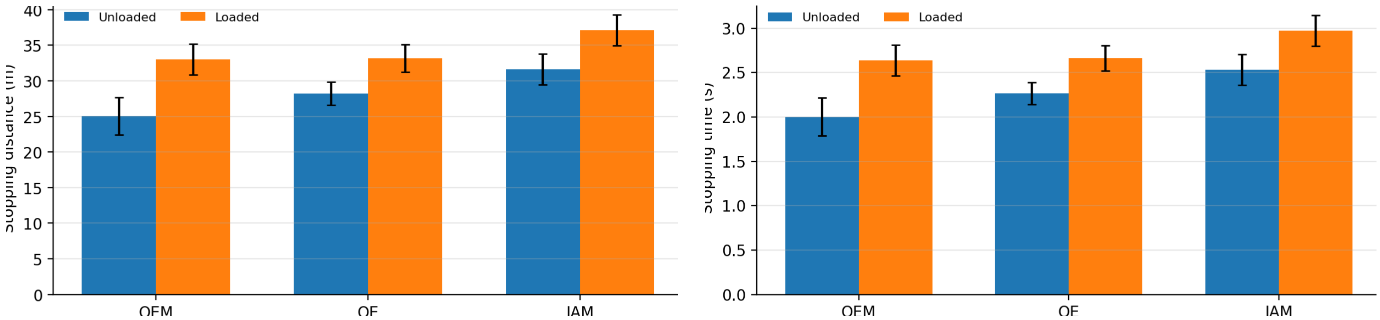

(a) Mean stopping distance.

(b) Mean stopping time.

Fig. 4: Mean stopping performance across pad categories and load states (mean ± SD, $n = 5$).

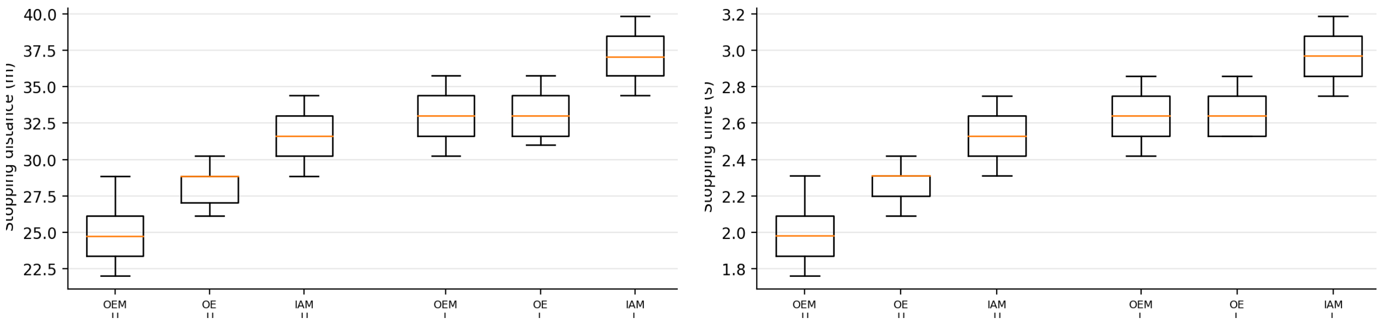

(a) Stopping distance distribution (boxplots).

(b) Stopping time distribution (boxplots).

Fig. 5: Dispersion across repetitions for distance and time (unloaded/loaded).

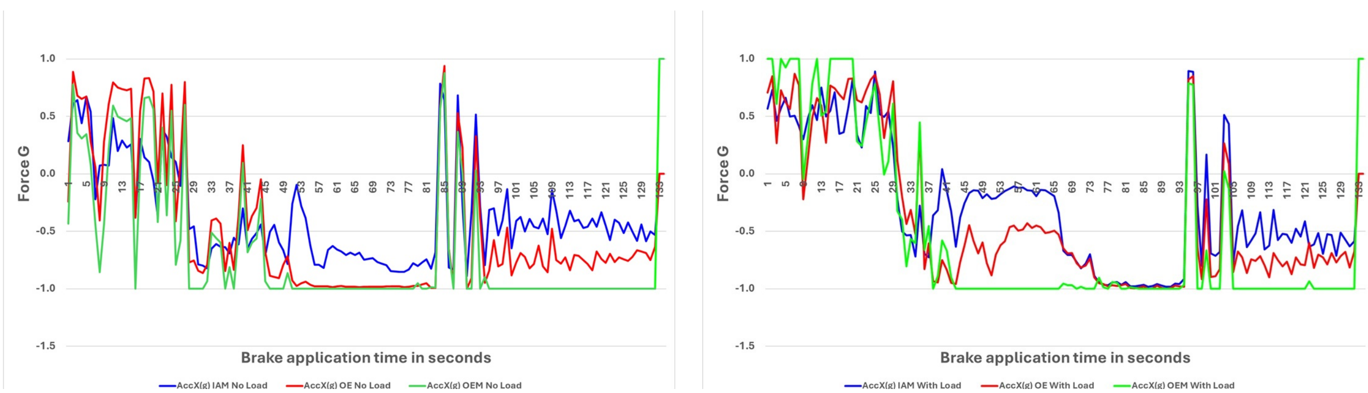

(a) Unloaded (OEM/OE/IAM).

(b) Loaded (OEM/OE/IAM).

Fig. 6: Representative longitudinal acceleration profiles (AccX in g) during full-stop tests for OEM, OE, and IAM pads under unloaded and loaded conditions.

the tire–road friction limit under ABS control. While the plateau deceleration magnitude is broadly similar across pads (bounded by friction and ABS), differences appear in the transient behavior (spikes and oscillations) and in the duration of sustained deceleration. These signatures align with the aggregate distance/time metrics: configurations that sustain stable deceleration over a shorter duration tend to achieve shorter stopping distance, whereas extended deceleration phases (especially under load) correspond to longer stops.

D. Comparison with Similar Studies

The present findings are consistent with the broader literature in two ways. First, they support the conclusion that market tier is an incomplete predictor of brake behavior. Balaji et al. found that a lower-cost OEM-category option could rank highly when fade, recovery, wear, and temperature metrics were jointly considered [10]. In the present road tests, the OE sample achieved loaded stopping distance and time very close to OEM, but it also reached substantially higher peak temperatures. Thus, equivalence in one metric did not imply

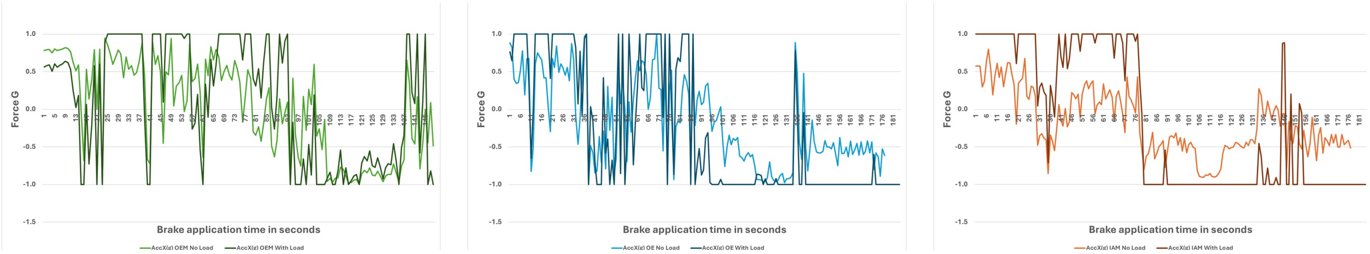

(a) OEM: unloaded vs. loaded. (b) OE: unloaded vs. loaded. (c) IAM: unloaded vs. loaded.

Fig. 7: Load effect on longitudinal acceleration profiles for each pad category (AccX in g).

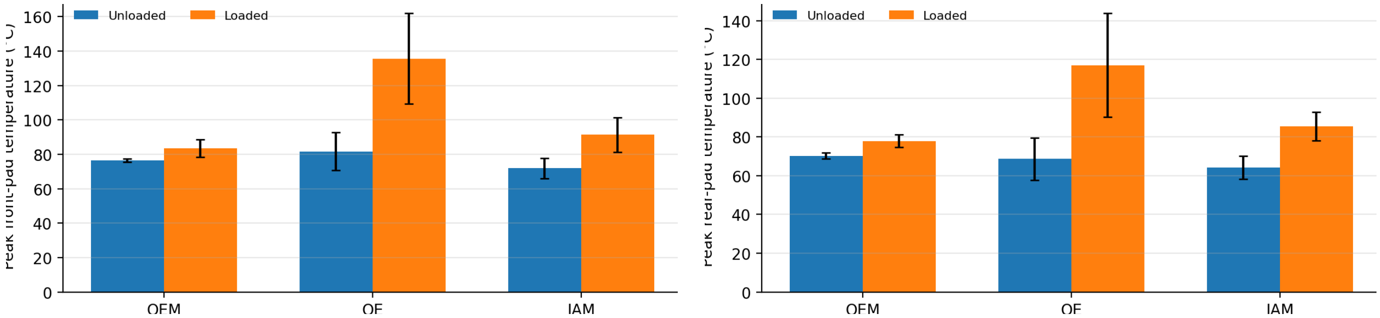

(a) Front peak temperature. (b) Rear peak temperature.

Fig. 8: Peak pad temperatures (front/rear) for each pad category and load state.

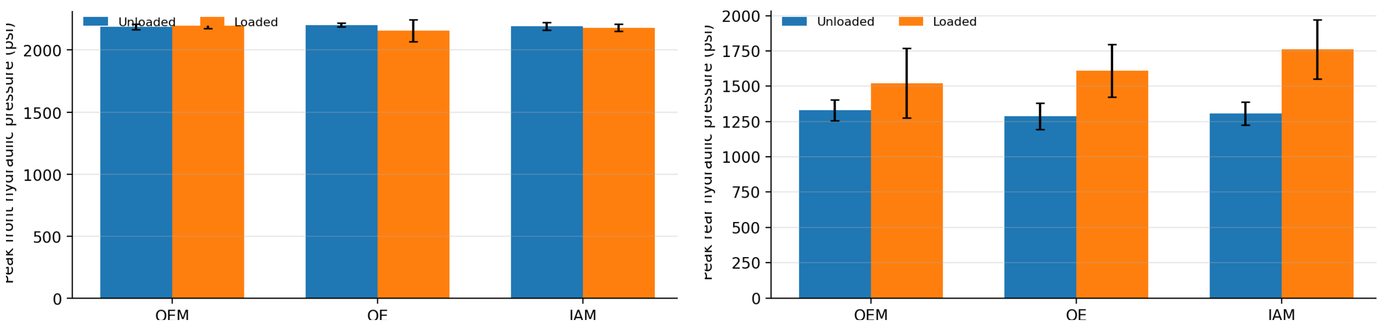

(a) Front peak pressure. (b) Rear peak pressure.

Fig. 9: Peak hydraulic pressures (front/rear) for each pad category and load state.

equivalence across all metrics.

Second, the results extend original-versus-aftermarket comparisons from bench or market studies to a full-vehicle context. Prior work by Neis et al. and Sethupathi et al. motivates comparative evaluation of replacement pads because fit compatibility does not guarantee equivalent friction behavior [11], [12], [13]. The IAM sample in this study confirms that point at the vehicle level: it had the longest mean stopping distance in both load states, even though it did not have the highest peak temperatures. Omar et al. reported that aftermarket brake-pad composition and price relationships can be nontrivial; similarly, the present IAM results show a mixed profile rather than a simple "low cost equals high thermal stress" interpretation [14]. Finally, the equivalent friction values in Table III should be interpreted as vehicle-level effective indicators derived from stopping distance, not as direct material coefficients, because tire friction, ABS control, pressure distribution, and load transfer are all active during the road tests [15].

E. Repeatability

Variability is a key outcome for safety-critical component comparisons. In this dataset, the coefficient of variation (CV) for stopping distance ranged from approximately 5.8 % to 10.5 % depending on configuration, with the unloaded OEM case showing the highest dispersion. To quantify uncertainty in the reported means, we also report the 95% confidence-interval (CI) half-width for the mean, computed as [18]:

$$\mathrm{CI}_{95} = t_{0.975,\,n-1}\,\frac{s}{\sqrt{n}}, \tag{10}$$

where s is the sample SD across repetitions and $n = 5$. Table V summarizes CV and CI half-widths for both distance

TABLE V: Dispersion and 95% CI half-width for the mean ($n = 5$). CV is reported in percent.

Pad	Load	CV_d	CI_d (m)	CV_t	CI_t (s)
OEM	U	10.5	3.27	10.5	0.26
OE	U	5.8	2.02	5.7	0.16
IAM	U	6.9	2.71	6.7	0.21
OEM	L	6.6	2.71	6.4	0.21
OE	L	5.9	2.43	5.3	0.17
IAM	L	5.8	2.67	5.7	0.21

TABLE VI: Qualitative rank summary (1 = best) across metrics (lower is better).

Pad	Load	Dist.	Time	$Temp_F$	$Press_F$
OEM	U	1	1	3	2
OE	U	2	2	2	1
IAM	U	3	3	1	3
OEM	L	1	1	2	2
OE	L	2	2	3	1
IAM	L	3	3	1	3

and time. For example, in the unloaded OEM case the CI half-widths are 3.27 m (distance) and 0.26 s (time), illustrating that small-sample campaigns can yield wide intervals even when mean differences appear meaningful. Such dispersion motivates reporting uncertainty and controlling additional factors (initial brake temperature window, surface friction monitoring, and speed tolerance) in future campaigns [7], [18].

F. Hydraulic Demand and Load Transfer

The measured pressure peaks can be interpreted through classical longitudinal load transfer. Under deceleration, the normal load shifts toward the front axle according to

$$\Delta F_z = \frac{m\,|a_x|\,h}{L}, \tag{11}$$

where m is vehicle mass, h is center-of-gravity height, and L is wheelbase. This increases available front tire traction and therefore the share of braking work assigned to the front axle under ABS. In a hydraulic system, brake torque scales approximately with line pressure ($T_b \propto P$), so pressure differences can reflect both friction-material behavior and control allocation between axles.

To summarize trade-offs across metrics, Table VI reports a simple rank ordering (1 = best) based on mean stopping distance and time (lower is better), as well as lower peak temperature and lower peak pressure (as proxies for thermal and hydraulic demand). While OEM leads distance/time in both load states, IAM tends to exhibit lower peak temperatures, whereas OE often shows slightly lower peak pressures. These observations emphasize that "best" depends on the objective: shortest stop, lowest thermal stress, or lowest hydraulic demand.

VI. Limitations and Future Work

This study focuses on straight-line dry-asphalt stops at a single nominal speed and does not include wet braking, fade sequences, or high-temperature recovery. A further limitation is that brand/model identifiers cannot be disclosed due to confidentiality; to mitigate this, the paper reports procurement channel and market-tier context for OEM, OE, and IAM samples. Future work will:

- Extend testing to wet surfaces and multiple speeds, including standardized fade/recovery cycles.
- Incorporate direct vehicle speed and distance instrumentation with explicit speed correction when needed (Eq. (5)).
- Add lining wear and particulate emission measurements to complement performance metrics.
- Perform statistical significance testing (ANOVA) across pad categories and load states with larger sample sizes [18].

VII. Conclusions

This paper presented a controlled comparison of OEM, OE, and IAM brake pads on a single light SUV under unloaded and loaded conditions using five repeated stops per configuration at 90 $\mathrm{km\,h^{-1}}$. The results are aligned with the study objectives. For stopping performance, OEM produced the shortest mean distance and time under unloaded conditions, whereas OEM and OE were nearly equivalent under loaded conditions. For load sensitivity, IAM showed the largest relative degradation versus OEM in both distance and time. For thermal/hydraulic behavior, OE reached the highest peak temperatures under load despite its close stopping performance to OEM, and rear-pressure variability increased in loaded tests. For repeatability, the reported SD, CV, and CI values show why dispersion must be reported alongside averages. Overall, the study supports category-level benchmarking of brake pads while recognizing that complete equivalence requires expanded standardized campaigns including wet braking, fade, endurance, and larger-sample statistical testing.

AI Use Disclosure & Author Responsibility Statement

AI Use Disclosure Statement. The authors declare that Artificial Intelligence tools were used for language editing, formatting assistance, citation-order checking, and LaTeX/PDF preparation support. All AI-assisted outputs were reviewed, validated, and edited by the authors.

Author Responsibility Statement. The authors assume full responsibility for the accuracy, originality, and integrity of all content in this manuscript, including AI-assisted components.

References

[1] SAE International, *SAE J299: Stopping Distance Test Procedure*. Warrendale, PA, USA, 2009.

[2] SAE International, *SAE J2909: Light Vehicle Dry & Wet Stopping Distance Test Procedure*. Warrendale, PA, USA, 2018.

[3] R. Limpert, *Brake Design and Safety*, 3rd ed. Warrendale, PA, USA: SAE International, 2011.

[4] J. Y. Wong, *Theory of Ground Vehicles*, 4th ed. Hoboken, NJ, USA: Wiley, 2008.

[5] P. J. Blau, *Friction Science and Technology: From Concepts to Applications*, 2nd ed. Boca Raton, FL, USA: CRC Press, 2008.

[6] K. Holmberg and A. Erdemir, “Influence of tribology on global energy consumption, costs and emissions,” *Friction*, vol. 5, no. 3, pp. 263–284, 2017.
[7] National Highway Traffic Safety Administration (NHTSA), *Brake Testing Methodology Study: Driver Effects Testing*. U.S. Department of Transportation, 1999.
[8] ISO, *ISO 26867:2009 Road Vehicles—Brake Lining Friction Materials: Friction Behaviour Assessment for Automotive Brake Systems*. Geneva, Switzerland, 2009.
[9] SAE International, *SAE J2522: Dynamometer Global Brake Effectiveness (AK Master)*. Warrendale, PA, USA, 2014.
[10] P. Balaji, B. S. Rajan, K. Sathickbasha, J. K. Katiyar, P. B. Sethupathi, and K. A. Ahmed, “A comparative study of original equipment manufacturer brake pads using tribological testing and hybrid ranking for enhanced decision making and cost effectiveness,” *Proc. Inst. Mech. Eng., Part J: J. Eng. Tribol.*, vol. 238, no. 5, pp. 483–499, 2024, doi: 10.1177/13506501231223593.
[11] P. D. Neis, N. F. Ferreira, and J. C. Poletto, “Comparative evaluation between original and aftermarket brake pads,” *SAE Technical Paper* 2015-36-0503, 2015, doi: 10.4271/2015-36-0503.
[12] P. D. Neis, N. F. Ferreira, and J. C. Poletto, “A comparative analysis of original and aftermarkets brake pads sold in the Brazilian market,” *J. Braz. Soc. Mech. Sci. Eng.*, vol. 38, pp. 1935–1945, 2016, doi: 10.1007/s40430-015-0440-3.
[13] P. B. Sethupathi, J. Chandradass, and M. A. Saibalaji, “Comparative study of disc brake pads sold in Indian market—impact on safety and environmental aspects,” *Environ. Technol. Innov.*, vol. 21, p. 101245, 2021, doi: 10.1016/j.eti.2020.101245.
[14] A. Omar, F. Lamin, and N. Mohamed, “Comparative study of brake pads in Malaysian automotive aftermarket,” *Int. J. Crashworthiness*, vol. 23, no. 2, pp. 144–150, 2018, doi: 10.1080/13588265.2016.1221372.
[15] M. Kchaou, A. Sellami, J. Fajoui, R. Kus, R. Elleuch, and F. Jacquemin, “Tribological performance characterization of brake friction materials: What test? What coefficient of friction?” *Proc. Inst. Mech. Eng., Part J: J. Eng. Tribol.*, vol. 233, no. 1, pp. 214–226, 2019, doi: 10.1177/1350650118764167.
[16] M. Eriksson, A. Lundqvist, and S. Jacobson, “A study of the influence of humidity on the friction and squeal generation of automotive brake pads,” *Proc. Inst. Mech. Eng., Part D: J. Automobile Eng.*, vol. 215, no. 3, pp. 329–342, 2001, doi: 10.1243/0954407011525674.
[17] WitMotion, “IMU/GNSS module datasheet (TTL serial, tri-axial acceleration and angular rate),” vendor technical documentation, accessed 2026.
[18] D. C. Montgomery, *Design and Analysis of Experiments*, 9th ed. Hoboken, NJ, USA: Wiley, 2017.